Journal of Integrative Agriculture 2026, 25(9): 3703–3714

Available online at ScienceDirect

Journal of Integrative Agriculture

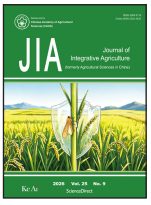

RESEARCH ARTICLE

Proton-responsive SlSTOP1–SlFRDL1 regulatory pathway modulates citrate-driven iron acquisition in tomato roots

Huihui Zhu[1*], Liqiong Jia[1*], Yuzhi Bai[1], Junqiang Xu[1], Xulu Luo[1], Wei Fan[1], Weiwei Chen[2#], Jianli Yang[1#]

[1] *Key Laboratory of Vegetable Biology of Yunnan Province, College of Landscape and Horticulture, Yunnan Agricultural University, Kunming 650201, China*

[2] *College of Life and Environmental Sciences, Hangzhou Normal University, Hangzhou 311121, China*

Highlights

- Iron deficiency induces organic acids and proton exudation to solubilize sparingly available iron.
- Citric acid exhibits superior iron solubilization efficacy at weakly acidic pH.
- SlSTOP1 binds to the promoter of *SlFRDL1* and activates its transcription, thereby mediating the citrate exudation triggered by iron deficiency.
- SlSTOP1–SlFRDL1 regulatory pathway is active in acidic pH but inactive in alkaline pH.

Abstract

The composition and function of root exudates in rhizosphere iron (Fe) mobilization are significantly influenced by environmental pH conditions. While the role of organic acids in Fe solubilization is well-recognized, the molecular mechanisms underlying this pH-dependent process remain poorly understood. Here, we demonstrate that under weakly acidic conditions, proton excretion alone is insufficient to solubilize sparingly soluble Fe. Instead, a pH-dependent ligand specificity emerges as a critical factor in Fe mobilization. Notably, within the pH range of 5.0–6.0, citric acid exuded by roots exhibits superior Fe solubilization efficacy compared to oxalic acid and malic acid. We identified *SlFRDL1*, a gene induced by Fe deficiency, as a key player in this process. *SlFRDL1* encodes a plasma membrane-localized protein with citrate permeability, as confirmed by its functional expression in *Xenopus* oocytes. Knockout mutants of *SlFRDL1* displayed exacerbated Fe deficiency symptoms, which were associated with a significant reduction in citrate secretion from roots. Furthermore, we discovered that SlSTOP1, a transcription factor, binds to the promoter region of *SlFRDL1* and activates its expression. *Slstop1* mutants exhibited leaf chlorosis symptoms similar to those observed in *Slfrdl1* mutants, highlighting the functional interplay between these two genes. Interestingly, while Fe deficiency triggers the FER-mediated Fe uptake system under both acidic and alkaline conditions, the SlSTOP1–SlFRDL1 module is specifically activated only in acidic environments. This pH-specific regulation underscores the importance of the SlSTOP1–SlFRDL1 pathway in root-mediated Fe solubilization under acidic conditions.

Keywords: citrate exudation, iron (Fe) mobilization, pH, SlFRDL1, SlSTOP1

1. Introduction

Iron (Fe) is an essential micronutrient for plant growth and development, and plays an important role in fundamental physiological processes such as chlorophyll synthesis, photosynthetic electron transfer and oxidoreductase activity regulation (Liang 2022). However, in calcareous soils or alkaline environments, Fe mainly exists in the form of insoluble trivalent oxides or hydroxides. Even at neutral or weakly acidic soil environments, Fe is prone to form sparingly soluble Fe(III)-phosphate ($FePO_4$) and hydroxides. Therefore, Fe bioavailability rarely meets the demand of plants, which results in young leaf chlorosis, growth retardation, and yield

Received 19 April 2025; Received in revised form 15 July 2025; Accepted 25 September 2025; Available online 31 December 2025
[#]Correspondence Jianli Yang, E-mail: yangjianli@zju.edu.cn; Weiwei Chen, E-mail: 15858223807@163.com
[*]These authors contributed equally to this study.

doi: 10.1016/j.jia.2025.12.072

loss in plants (Mori 1999). It has been estimated that about 30% of the world's arable soils suffer from Fe deficiency, resulting in billions of dollars in crop economic losses each year (Briat *et al.* 2015). To cope with this challenge, plants have developed two main types of adaptive mechanisms over a long period of evolution, namely Strategy I and Strategy II (Kobayashi and Nishizawa 2012). While graminaceous plants (Strategy II) acquire Fe by increasing the solubility of rhizosphere Fe mainly through the secretion of phytosiderophores, non-graminaceous plants (Strategy I) rely on secretion of root exudates to solubilize and reduction of ferric Fe (Fe^{3+}) to ferrous Fe (Fe^{2+}), thereby facilitating Fe uptake (Römheld and Marschner 1986). Therefore, root exudates play an important role in Fe deficiency response in both Strategy I and Strategy II plants.

Depending on the duration of stress and plants species, Fe deficiency induces the secretion of a variety of compounds such as organic acids, phenolic compounds, proton, and phytosiderophores from plant roots. In Strategy I plants such as *Arabidopsis* (*Arabidopsis thaliana*), Fe deficiency activates plasma membrane H^+-ATPase (AHA2), which acidifies the rhizosphere to solubilize Fe and improve ferric chelate reductase (FCR) activity (Santi and Schmidt 2009). Fe deficiency also induces secretion of phenylpropanoid-derived coumarins (Rosenkranz *et al.* 2021). Findings from numerous studies have shown that coumarins such as scopoletin, fraxetin, and sideretin could be secreted into rhizosphere where these compounds could either chelate Fe^{3+} or reduce Fe^{3+} directly (Schmid *et al.* 2014; Rajniak *et al.* 2018; Tsai *et al.* 2018). In red clover (*Trifolium pratense*), phenolic compounds secreted by the roots also promote apoplastic Fe reutilization (Jin *et al.* 2007), a process has been regarded as an important response to improve Fe use efficiency (Zhu *et al.* 2023, 2024b). On the other hand, graminaceous Strategy II plants secrete phytosiderophores that bind Fe^{3+} with high affinity and are directly transported across membranes (Nozoye *et al.* 2011). Studies on wheat have found that root-secreted phytosiderophores have a strong effect on rhizosphere Fe activation (Awad *et al.* 1994; Oburger *et al.* 2014). On the other hand, although it has long been recognized that root organic acids secretion is related to rhizosphere Fe solubilization (Chen *et al.* 2017), the molecular mechanism by which Fe deficiency regulates secretion of organic acids is still poorly studied.

Since the isolation and characterization of genes encoding citrate transporter proteins from sorghum and barley, extensive research has demonstrated their involvement in citrate exudation under conditions of metal toxicity and phosphorus deficiency (Yang *et al.* 2019). Notably, these citrate transporter proteins also play a crucial role in iron (Fe) translocation through the xylem in plants. For instance, in *Arabidopsis*, the citrate transporter protein FRD3 facilitates citrate transport into the xylem, where it forms chelates with Fe, thereby enabling Fe transport from roots to shoots (Green and Rogers 2004; Durrett *et al.* 2007). Similarly, barley (*Hordeum vulgare*) HvAACT1 and FRD3 homologs in soybean (*Glycine max*) have been shown to perform analogous functions in promoting Fe xylem translocation (Rogers *et al.* 2009; Fujii *et al.* 2012). However, the potential role of citrate transporter proteins in Fe deficiency-induced citrate exudation remains unexplored. Given the significant potential of such exudation for enhancing rhizosphere Fe dissolution (Jones *et al.* 1996), further investigation into this aspect would be particularly valuable.

As a globally important cash crop, tomato cultivation is often exposed to Fe deficiency stress caused by alkaline or calcareous soils (Zhu *et al.* 2022, 2023, 2024b). Especially, as a calcicole species, tomato requires a large amount of Ca fertilizers, which results in increase of environmental pH, thereby exacerbating the immobilization of Fe, causing interveinal leaf chlorosis, fruit stunting, and yield loss of tomato. Although tomato is a typical Fe-deficiency-adapted dicotyledonous plant, the ability of its root system to secrete organic acids varies significantly among cultivars, and the weakening of Fe-deficiency response mechanisms in some cultivars due to long-term domestication further exacerbates the risk of Fe-nutritional deficiencies in production (Briat *et al.* 2015). Studies on response of tomato to Fe deficiency have revealed physiological and molecular bases of Fe acquisition processes under Fe limited condition (Jin *et al.* 2011; Chen *et al.* 2022), but the mechanisms by which root exudates promote Fe mobilization are less understood.

In this study, we investigated the role of tomato root exudates in solubilizing insoluble Fe by hydroponics and compared pH-ligand synergy for Fe solubilization. We found citrate has great potential in increasing Fe solubilization at pH range between 5.0–6.0. Further, we functionally characterized *SlFRDL1* in terms of Fe-deficiency-induced citrate secretion, and elucidated the SlSTOP1-regulated mechanism of *SlFRDL1* expression. Our results not only reveal the molecular basis of root exudates-mediated Fe uptake in tomato, but also lay the foundation for breeding new Fe-deficiency-tolerant tomato varieties through gene editing or molecular marker-assisted breeding, which is of great significance for alleviating the agricultural losses caused by soil Fe-deficiency.

2. Materials and methods

2.1. Plant materials and treatment conditions

The tomato (*Solanum lycopersicum*) cultivar Ailsa Craig (AC) and *Slstop1* mutants were described in our previous study (Zhu *et al.* 2024a). SlFRDL1-KO constructs were created by selecting two specific sgRNAs using the CRISPR-PLANT online program, which were then incorporated into a CRISPR/Cas9-mediated knockout vector. All recombinant constructs were introduced into the AC background *via Agrobacturium*-mediated leaf disk transformation, and homozygous lines were screened. The surface-sterilized seeds were germinated in plastic petri dish containing solidified 1/5 Hoagland nutrient medium (pH 5.5) and 1% (w/v) agar. Seedlings with about 3–4-cm root length were transferred to containers with 1/5 Hoagland nutrient solution for 1 week. Then, the acclimatized seedlings were treated with Fe sufficiency (+Fe), Fe deficiency (–Fe) and Fe deficiency with $FePO_4$ supplementation (–Fe+$FePO_4$) with pH 6.5 condition for 2 weeks, and the treatment solution was renewed every other day. Additionally, we also supplemented

with exogenous citrate to investigate phenotypic rescue in *Slstop1* and *Slfrdl1* mutants under Fe deficiency with $FePO_4$ supplementation (–Fe+$FePO_4$) for pH 6.5 condition.

2.2. Leaf morphological analysis and Fe determination

The young chlorotic leaves were photographed with a Nikon digital camera. The Chl content were estimated by immersing in 95% ethanol until completely bleached and then measured Chl *a* and Chl *b* with a spectrophotometer at 663 and 646 nm, respectively. The Fe content in hydroponic solution or *in vitro* $FePO_4$ dissolution assays was directly detected after filtration. For the Fe content in plants, samples were dried at 110°C and then digested in concentrated HNO_3 for 5 h at 160°C. The Fe contents were measured by ICP–MS (inductively coupled plasma–mass spectrometry; Agilent 7500ce, USA).

2.3. Rhizosphere acidification assays and organic acid determination

The pH in hydroponic nutrient solution was determined with pH meter. The visualization of rhizosphere acidification was used by pH indicator bromocresol purple and imaged with a Nikon digital camera. The oxalic acid, citric acid, and malic acid was detected by enzymatic methods as previous reported (Zhu *et al.* 2024a).

2.4. Total RNA extraction and reverse transcription quantitative real-time qPCR analysis

Total RNA was isolated from root tissues, and first-strand cDNA synthesis was performed using the FastQuant RT Kit with gDNA Eraser (Tiangen, China). Gene-specific primers (Appendix A) and SYBR Green chemistry (Toyobo) were then used for reverse transcription quantitative real-time PCR (RT-qPCR) on a Roche LightCycler 480 machine. The expression levels of specific genes were normalized relative to *ACTIN*. The primer pairs were listed in Appendix A.

2.5. Citrate permeability assay of SlFRDL1 in *Xenopus* oocytes

Citrate permeability of SlFRDL1 was determined in *Xenopus* oocytes as our previous report (Liu *et al.* 2018). The coding region of *SlFRDL1* or *SlFRDL1:GFP* fusion construct was amplified and inserted between the 5′ and 3′ UTRs of the *Xenopus β-globin* gene in a T7TS vector. cRNA was synthesized using a mMESSAGE mMACHINE high-yield capped RNA transcription kit (Ambion, America). cRNA microinjection were performed as previously described (Piñeros *et al.* 2008; Yang *et al.* 2011). In brief, 50 nL RNase-free water, or 50 nL SlFRDL-T7TS cRNA (1 ng nL^{-1}), and 50 nL SlFRDL-GFP-T7TS cRNA (1 ng nL^{-1}) were injected into oocytes, respectively. After 1-d culture, oocytes with or without *SlFRDL1* expression were injected with 50 nL of 2.5 mmol L^{-1} citrate. The oocytes were washed for 5 min in the ND96 bath solution contained (in mmol L^{-1}): NaCl (96), KCl (1) and $CaCl_2$ (1.8) (pH 5.0), and cultured in 1.5 mL (50 oocytes) of bath solution for 24 h. After treatment, bath solution was collected and the oocytes were homogenized with 1.5 mL of bath solution. Citrate content in bath solution and homogenates were assay enzymatically.

2.6. Luciferase activity reporter assay in *N. benthamiana*

The CDS sequence of *SlSTOP1* was inserted into the vector pCAMBIA1300 driven by the CaMV 35S promoter. The reporters were constructed by ligating the *SlFRDL1* promoter segments with motifs into the pGreenII0800-LUC vector. Subsequently, SlSTOP1 and segmented *SlFRDL1* promoter were co-expressed in *N. benthamiana* leaves through *Agrobacterium*-mediated infiltration, and luciferase (LUC) activity was measured using the Night SHADE LB 985 plant imaging system (Berthold).

2.7. Yeast one-hybrid analysis

The CDS sequence of *SlSTOP1* and the *SlFRDL1* promoter segments were inserted into pGADT7 and pAbAi vector, respectively. Pairs of plasmids were transformed into the yeast strain Y1HGold and grown on SD medium lacking Ura with 0–200 ng mL^{-1} aureobasidin A (AbA) at 30°C for 3 d.

2.8. Electrophoretic mobility shift assay

The *SlSTOP1* CDS was ligated into the *pCold-TF* vector to induce SlSTOP1 protein expression, and SlSTOP1 protein purification. Biotin-labeled probes and nonlabelled competitors are synthesized and then annealed as double-stranded DNA probes and competitors. An electrophoretic mobility shift assay (EMSA) was performed using a chemiluminescent EMSA kit following the manufacturer's instructions (Beyotime Biotechnology, China).

2.9. Statistical analysis

All data are presented as means±SD with at least three biological replicates in different assays. The statistical analyses were performed by Tukey's test or one-way analysis of variance, and statistically significant differences among treatments were determined at the $P \leq 0.05$ level.

3. Results

3.1. Root exudates play an essential role in Fe solubilization from $FePO_4$

Previous study has demonstrated that Fe deficiency-induced root secretion of organic acids can form stable complex with Fe only at pH<6.8 (Jones *et al.* 1996). As the major objective of this study lies in revealing regulatory role of organic acids in solubilizing Fe, the experimental conditions were set as pH 6.5 and the sparingly soluble Fe(III)-phosphate ($FePO_4$) used as the sole Fe source. We conducted a hydroponic experiment to investigate the mechanisms underlying root exudate-mediated Fe acquisition from ($FePO_4$) at initial pH of 6.5. The treatment solution was renewed every other day. After 14 d of treatment, $FePO_4$ supplementation (–Fe+$FePO_4$) effectively alleviated Fe deficiency-induced chlorosis compared with the Fe-deprived control (–Fe) (Fig. 1-A and B). Quantitative analysis revealed 1.6- and 4.6-fold increases in Fe accumulation in shoots and roots, respectively, under –Fe+$FePO_4$ treatment relative to the –Fe condition (Fig. 1-C and D), demonstrating active Fe acquisition from $FePO_4$ by tomato plants.

To differentiate between chemical dissolution and plant-

mediated Fe mobilization, we employed time-course monitoring of Fe concentration in the nutrient solution using ICP–MS. Throughout the 14-d experimental period, Fe remained undetectable (<0.001 ppm) in plant-free systems containing $FePO_4$, confirming the chemical stability of $FePO_4$ at pH 6.5. Remarkably, in plant-containing systems, soluble Fe concentrations were detected and exhibited a progressive increase starting from d 10. This temporal pattern correlated with root developmental stages showing enhanced exudate secretion. Our findings provide direct evidence that root exudates play an essential role in Fe solubilization from $FePO_4$. The delayed onset of Fe release (from d 10 onward) corresponds with the phenological progression of root maturation and exudation capacity, suggesting a plant-regulated mechanism rather than passive chemical dissolution.

3.2. pH-dependent ligand specificity in Fe solubilization

To determine whether $FePO_4$-induced Fe acquisition involves root exudate-mediated acidification, we systematically monitored pH dynamics in the hydroponic system. Nutrient solutions were replaced every 48 h to maintain initial pH 6.5, with pH measurements conducted 24 h post-replacement. A pronounced pH decrease emerged in the –Fe+$FePO_4$ treatment by d 8 (5.3±0.2), preceding the pH decline observed in the –Fe control (d 10, 5.8±0.1), while the +Fe treatment was maintained pH values between 5.8–6.3, which were significantly higher than –Fe or –Fe+$FePO_4$ (Fig. 2-A). Notably, the –Fe+$FePO_4$ system exhibited greater acidification than the –Fe condition by d 8 ($P<0.05$). Complementary rhizosphere pH imaging using bromocresol purple revealed intensified acidification halos around roots in –Fe+$FePO_4$ plants compared to –Fe controls (Fig. 2-B), supporting the critical role of localized proton extrusion in facilitating $FePO_4$ solubilization.

Given the dual role of organic acids in Fe chelation and pH modulation, we quantified root-secreted anions *via* enzymatic method (Zhu *et al.* 2024a). Tomato roots predominantly released oxalate (0.19±0.05 nmol per root tip) and citrate (0.05±0.01 nmol per root tip) under –Fe+$FePO_4$ conditions, representing 2.8- and 2.4-fold increases over +Fe controls, respectively (Fig. 2-C). Malate secretion remained below detection limits across treatments, excluding its functional involvement. We further measured citrate efflux after 2, 6, 10, and 14 d of Fe deficiency treatment. A significant increase in citrate secretion was observed from d 6, which progressively intensified with prolonged deficiency (Appendix B).

To dissect the relative contributions of protons *vs.* organic acids, we conducted *in vitro* $FePO_4$ dissolution assays under controlled pH conditions. We found distinct ligand-specific patterns with respect to Fe solubility. Fe solubility was negligible above pH 5.0 with the contribution of HCl. Oxalate exhibited the best Fe dissolution at pH<5.0

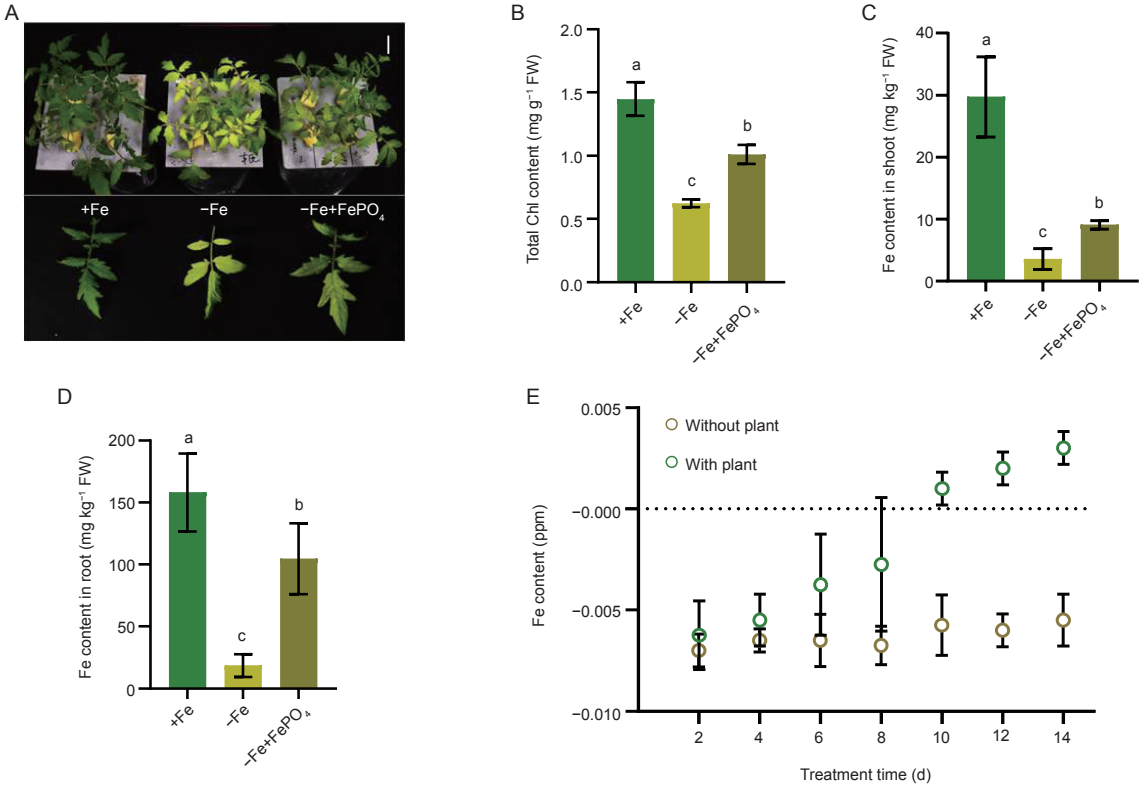

Fig. 1 Root exudates-mediated utilization of sparingly soluble Fe improved Fe nutrition in tomato. A, the leaf chlorosis phenotype of plants grown in Fe sufficiency (+Fe), or Fe deficiency (–Fe), or Fe deficiency supplied with $FePO_4$ (–Fe+$FePO_4$). B, the total chl content under +Fe, –Fe, or –Fe+$FePO_4$. C and D, the Fe content in shoots (C) and roots (D) under +Fe, –Fe, or –Fe+$FePO_4$. E, influence of plant roots on Fe content in the hydroponic solution under –Fe+$FePO_4$ condition. Tomato (cv. AC) seedlings were cultured hydroponically for 14 d, and the treatment solution was renewed every other day. All data are presented as means±SD (n=4 biological replicates) with different letters indicating significant differences among treatments at P≤0.05 level by Tukey's test.

(0.17 ppm) or pH>6.0 (0.06 ppm). However, citrate showed maximal efficacy (0.104 ppm Fe) within the pH 5.0–5.8 range (Fig. 2-D). Notably, the rhizosphere pH window observed in planta (5.0–6.0, Fig. 2-A) aligns with citrate's optimal chelation capacity, suggesting its predominant role in $FePO_4$ mobilization. This pH-ligand synergy likely underlies the enhanced Fe acquisition and chlorosis recovery in –Fe+$FePO_4$ plants.

3.3. SlFRDL1-mediated citrate secretion is involved in Fe solubilization

Root citrate efflux in plants is primarily regulated by multidrug and toxic compound extrusion (MATE) family transporters (Yang *et al.* 2019). In tomato, three MATE homologs, *SlFRDL1*, *SlFRDL2*, and *SlFRDL3*, were previously identified as putative citrate transporters (Jin *et al.* 2022). Our expression analysis revealed *SlFRDL1* as the dominant isoform, exhibiting root-specific expression and strong induction under Fe-deficient conditions (Fig. 3-A). Time-course experiments further demonstrated significant upregulation of *SlFRDL1* transcripts after 48 h of Fe deprivation (Fig. 3-B).

To resolve the subcellular localization of SlFRDL1, we transiently expressed a SlFRDL1:GFP fusion construct in tomato protoplasts. Confocal microscopy revealed complete colocalization of GFP fluorescence with a plasma membrane RFP marker (Fig. 3-C). Functional characterization in *Xenopus laevis* oocytes confirmed plasma membrane targeting of the SlFRDL1:GFP fusion protein (Fig. 3-D). Electrophysiological assays demonstrated more citrate efflux from SlFRDL1-expressing oocytes compared to controls (Fig. 3-E), corroborated by a corresponding reduction in

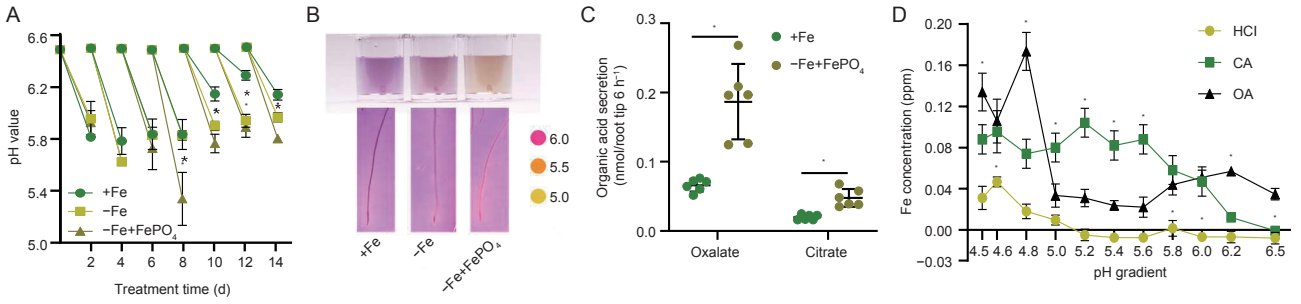

Fig. 2 The contribution of proton and organic acids to solubilization of Fe from $FePO_4$. A, the pH value in the hydroponic solution with Fe sufficiency (+Fe), Fe deficiency (–Fe), or Fe deficiency supplied with $FePO_4$ (–Fe+$FePO_4$). B, the rhizosphere acidification under +Fe, –Fe, or –Fe+$FePO_4$. C, the oxalate and citrate secretion under +Fe or –Fe+$FePO_4$ conditions. D, chemical dissolution assay $FePO_4$ by protons, citric acid (CA), and oxalic acid (OA) under different pH gradients. Means±SD (*n*=6 biological replicates) with asterisks indicated significant differences among treatments at $P \leq 0.05$ level by Tukey's test.

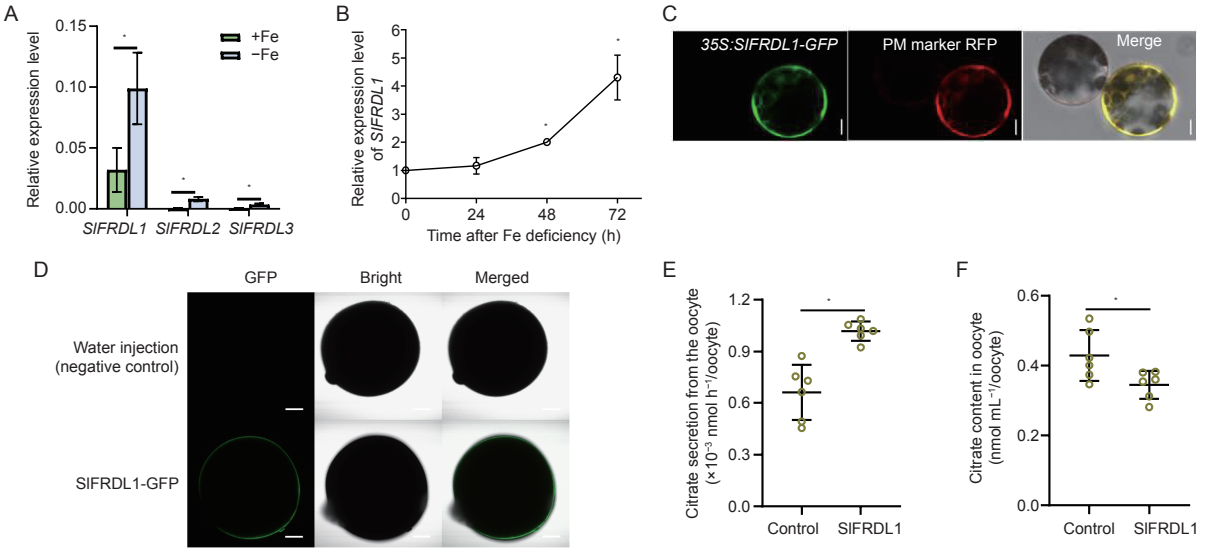

Fig. 3 Functional characterization of tomato SlFRDL1. A, the expression of three *SlFRDL* genes in AC roots in response to Fe deficiency. B, a time-course expression analysis of *SlFRDL1* in response to Fe deficiency. 14 d-old seedling roots with or without Fe deficiency for 0, 24, 48 and 72 h were extracted for determining gene expression. C, subcellular localization of SlFRDL1. 35S:SlFRDL1-GFP vector was expressed in tomato protoplasts for 48 h, and then GFP signal was observed with a laser confocal microscope. Scale bars=10 μm. D, cellular localization of SlFRDL1-GFP expressed in *Xenopus* oocytes. Bars=0.2 mm. E and F, the citrate secretion from the *Xenopus* oocytes (E) and citrate content in the *Xenopus* oocytes (F). Data are presented as means±SD (*n*=6 biological replicates). Asterisks above the bars indicate statistical differences at $P<0.05$ level by Tukey's test.

intracellular citrate levels (Fig. 3-F). These complementary results provide direct evidence for SlFRDL1-mediated citrate transport activity.

To examine the role of SlFRDL1 in Fe mobilization, we analyzed two independent CRISPR-Cas9-generated *SlFRDL1* knockout lines (*Slfrdl1*#4 and *Slfrdl1*#6) (Appendix C). Under Fe-sufficient conditions (+Fe), no visible phenotypic differences were observed between wild-type (AC) and *SlFRDL1* mutants. However, under Fe limitation with $FePO_4$ (–Fe+$FePO_4$), both knockout lines displayed pronounced interveinal chlorosis (Fig. 4-A), accompanied by 35–40% reductions in total chlorophyll content relative to AC (Fig. 4-B).

Fe quantification revealed subtle but significant shoot Fe reductions in mutants under +Fe conditions (AC: 29.7±6.47 mg kg^{-1} FW *vs.* mutants: 21.1–21.8 mg kg^{-1} FW, P<0.05), suggesting that SlFRDL1 also play role in regulating Fe translocation from roots to shoots. The –Fe+$FePO_4$ treatment exacerbated these differences, with mutant shoots and roots accumulating 56% and 67% less Fe, respectively, than AC plants (Fig. 4-C and D). Root exudate profiling demonstrated that *SlFRDL1* disruption reduced constitutive citrate secretion by 51% under +Fe conditions (AC: 0.044±0.007 nmol per root tip *vs.* mutants: 0.022–0.023 nmol per root tip). Crucially, $FePO_4$-induced citrate secretion, which increased 3.1-fold in AC roots, was virtually abolished in both mutants (Fig. 4-E). The impaired Fe acquisition in mutants triggered amplified molecular responses, as evidenced by 2.5- to 3.8-fold upregulation of the Fe deficiency markers *SlFRO1* (ferric chelate reductase) and *SlIRT1* (iron-regulated transporter) compared to AC (Fig. 4-F and G).

3.4. SlSTOP1 is involved in SlFRDL1-mediated Fe acquisition in tomato

Building on the established roles of AtSTOP1 in *Arabidopsis* and OsART1 in rice in activating MATE transporters during aluminum stress (Liu *et al.* 2009; Yokosho *et al.* 2016), we investigated whether the tomato homolog SlSTOP1 governs *SlFRDL1* induction under Fe limitation. Bioinformatic screening of the *SlFRDL1* promoter revealed seven putative cis-acting elements matching the conserved STOP1-binding motif GGN (T/G/A/C)V(C/A/G)S(C/G) (Tsutsui *et al.* 2011). These elements were distributed across seven promoter fragments (P1–P7, Fig. 5-A). Transient dual-luciferase assays in *N. benthamiana* leaves demonstrated that co-expression of *SlSTOP1* with promoter-reporter constructs specifically activated the P5, P6, and P7 fragments (LUC/REN ratio, P<0.01), with P6 showing maximal responsiveness (Fig. 5-B and D). Yeast one-hybrid assays further validated *SlSTOP1* binding to three promoter subregions (Y3–Y5, corresponding to P5–P7 in Fig. 5-A), with strongest interaction observed for the Y4 fragment (Fig. 5-E). Focusing on the P6 motif (Y4 subfragment), competitive EMSA using purified His-tagged SlSTOP1 protein demonstrated dose-dependent binding to the biotin-labeled wild-type probe (Fig. 5-F). Binding affinity decreased dramatically in the presence of 100× unlabeled competitor and was abolished when critical nucleotides in the core motif were mutated (Fig. 4-F, right panel).

To further confirm that SlSTOP1-regulated *SlFRDL1* expression is related to Fe acquisition, we observed leaf chlorosis phenotype in AC and two *Slstop1* lines under +Fe or –Fe+$FePO_4$ condition. Similar to the phenotype of two *Slfrdl1* lines, two *Slstop1* lines displayed greater leaf chlorosis than

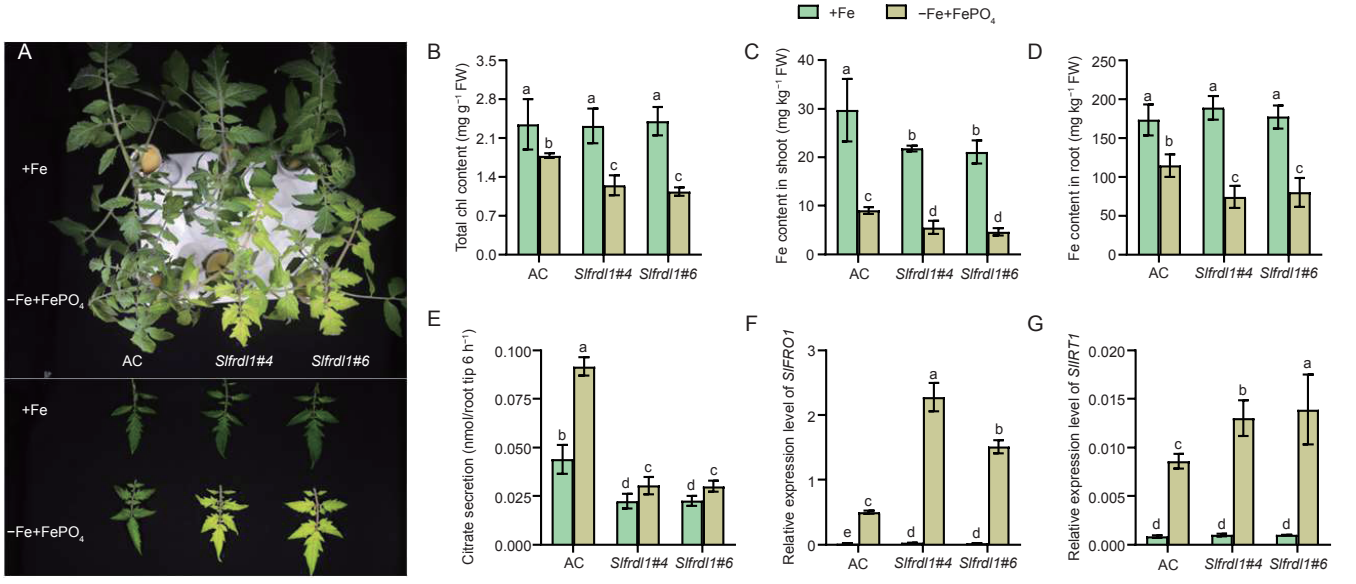

Fig. 4 SlFRDL1 is involved in rhizosphere Fe mobilization. A, the leaf chlorosis phenotype under Fe sufficiency (+Fe) or Fe deficiency supplied with $FePO_4$ (–Fe+$FePO_4$) conditions. B, the total chl content under +Fe or –Fe+$FePO_4$. C and D, the Fe content in shoots (C) and roots (D) under +Fe or –Fe+$FePO_4$. E, the citrate secretion from AC plants and two *SlFRDL1* KO lines under +Fe or –Fe+$FePO_4$ conditions. F and G, the gene expression of *SlFRO1* (F) and *SlIRT1* (G) in AC plants and two *SlFRDL1* KO lines under +Fe or –Fe+$FePO_4$ conditions. Tomato seedlings were cultured hydroponically for 14 d, and the treatment solution was renewed every other day. AC, Ailsa Craig. All data are presented as means±SD (n=4 biological replicates) with different letters indicating significant differences among treatments at P≤0.05 level by ANOVA analysis.

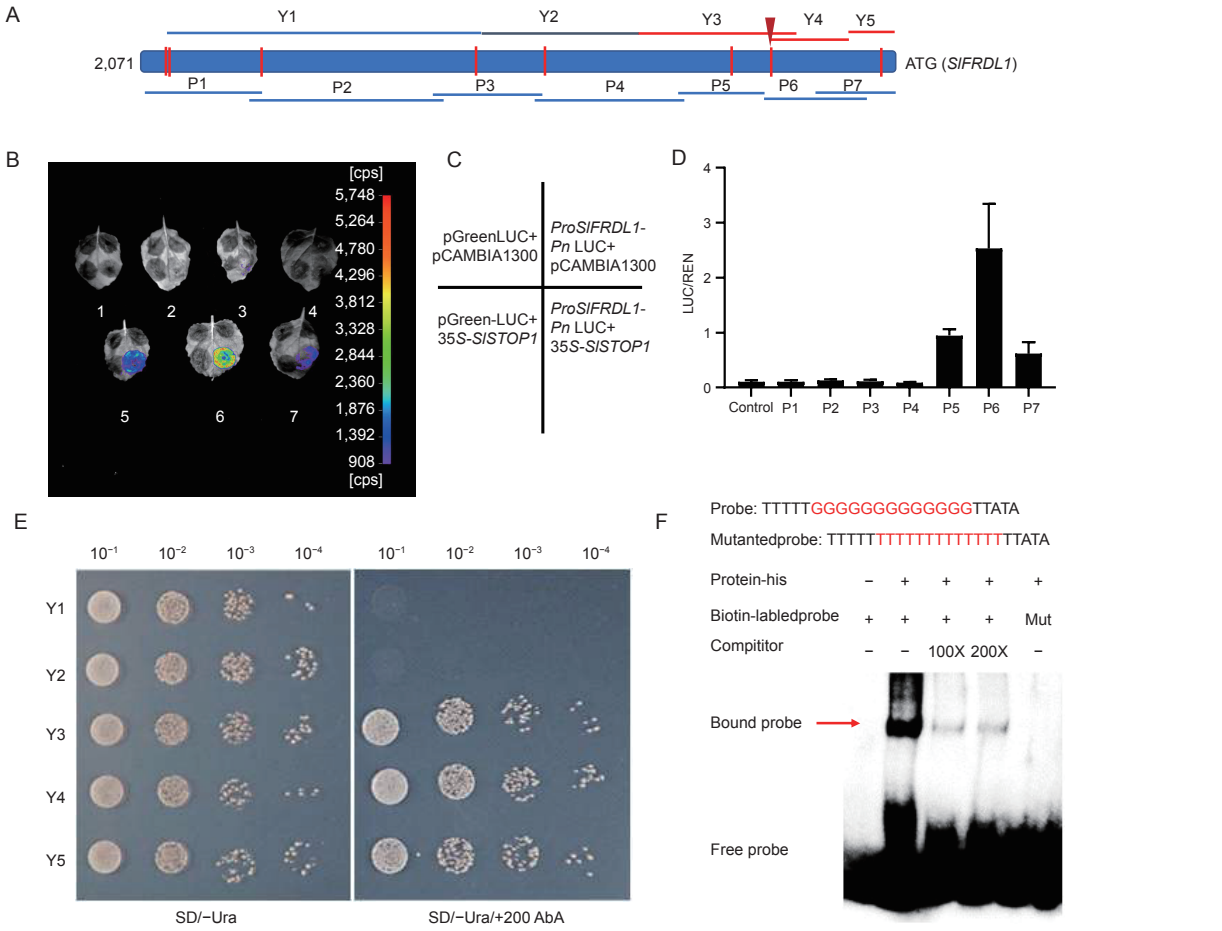

Fig. 5 SlSTOP1 directly binds to the *SlFRDL1* promoter. A, schematic diagram of the *SlFRDL1* promoter fragments used for transcriptional activity assay and Y1H assay. Red vertical line indicated the motif location. Red inverted triangle indicated the probe used in (F) location. B and C, the interactions between SlSTOP1 and the fragments of *SlFRDL1* promoter by transient luciferase assay in *Nicotiana benthamiana* leaves. The full-length sequence of SlSTOP1 protein was inserted into the effector vector (pCAMBIA1300) and *SlFRDL1* promoter fragments were separately inserted into luciferase (LUC)-based reporter vector (pGreenII0800 LUC). The effector and reporter were transiently co-expressed in *N. benthamiana* leaves by *Agrobacterium tumefaciens*-mediated transformation. The colored scale bars indicate the luminescence intensity (counts s^{-1}). D, relative luminescence intensities were calculated using Night SHADE LB 985 (Berthold, Germany). E, Y1H analysis of the transcriptional regulation of *SlFRDL1* by SlSTOP1. The plasmids of pAbAi-SlFRDL1 (promoter fragments from Y1 to Y5) and pGAD-SlSTOP1 were introduced into yeast strain Y1HGold, which was cultured on medium without Ura but containing aureobasidin A (AbA). F, the gel-shift assay identified the binding efficiency of SlSTOP1 to *SlFRDL1* promoter. The *SlFRDL1* promoter containing *cis*-acting element or mutated element in P6 fragment were labeled with biotin. Unlabeled DNA fragments were used as competitors.

AC plants under –Fe+$FePO_4$ condition (Fig. 6-A), which was consistent with lower chlorophyll content in two *Slstop1* lines than AC plants (Fig. 6-B). Notably, like in *Slfrdl1* lines the Fe content in shoots of two *Slstop1* lines was significantly lower than AC shoots under either +Fe sufficiency or –Fe+$FePO_4$ condition (Fig. 6-C), but not significant difference in root Fe content was observed between AC and two *Slstop1* lines (Fig. 6-D). We also determined *SlFRDL1* expression in AC and two *Slstop1* lines, and found that the root expression of *SlFRDL1* in two *Slstop1* lines was significantly lower than that in AC plants under –Fe+$FePO_4$ (Fig. 6-E). Moreover, exogenous citrate supplementation rescued the chlorosis phenotype of *Slstop1* and *Slfrdl1* mutants under Fe deficiency (Appendix D). These results demonstrate that SlSTOP1 positively contributes to Fe solubilization by regulation of *SlFRDL1*-mediated citrate secretion.

3.5. Activation of SlSTOP1–SlFRDL1 module under Fe deficiency is pH-dependent

Previous studies have established that acidic environments are essential for STOP1 accumulation and activation under various stress conditions (Huang and Ma 2024). To investigate whether this acidic requirement extends to *SlFRDL1* induction during Fe deficiency, we examined the SlSTOP1–SlFRDL1 regulatory module. Initial analysis of *SlSTOP1pro:GUS* transgenic tomato roots revealed comparable GUS activity between +Fe and –Fe+$FePO_4$ conditions (Fig. 7-A), consistent with RT-PCR results showing no significant differences in *SlSTOP1* transcript levels (Fig. 7-B). However, confocal microscopy demonstrated enhanced SlSTOP1-GFP fluorescence intensity under –Fe+$FePO_4$ treatment compared to +Fe conditions (Fig. 7-C

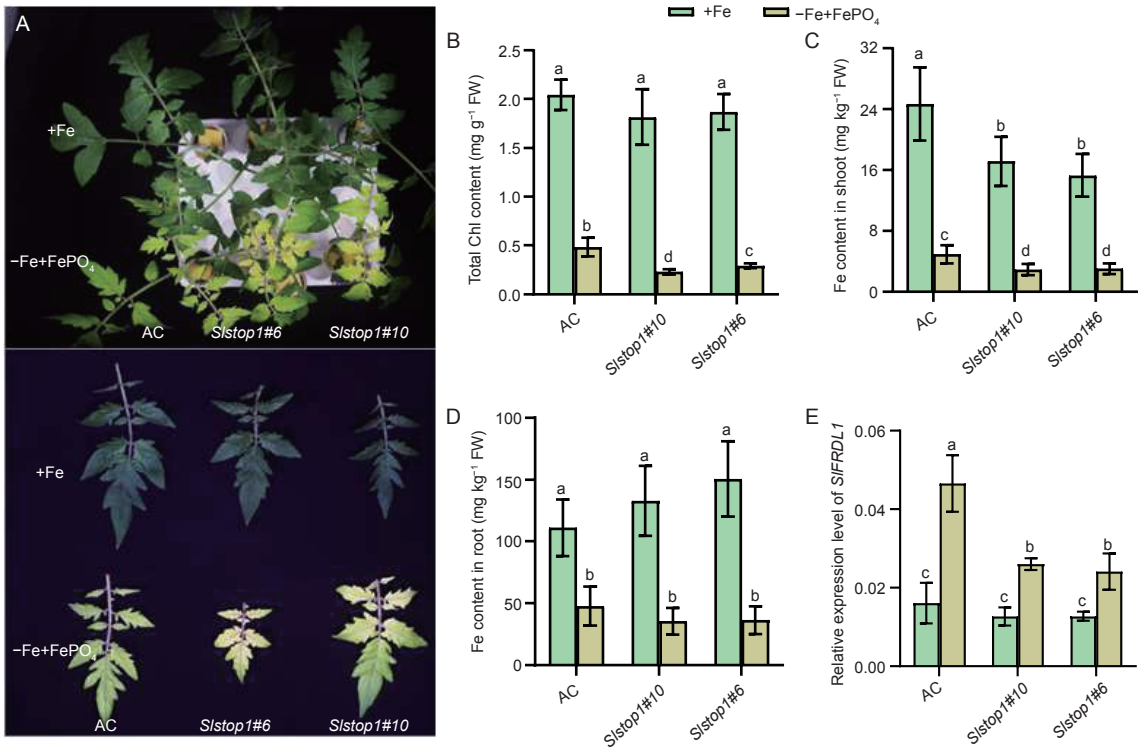

Fig. 6 SlSTOP1 is involved in rhizosphere Fe mobilization. A, the phenotype of tomato leaves in AC and two *SlSTOP1* KO lines subjected to Fe sufficiency (+Fe) or Fe deficiency condition supplied with $FePO_4$ (–Fe+$FePO_4$). B, the total Chl content in (A). C and D, the Fe content in shoot (C) and root (D) of AC and two *SlSTOP1* KO lines under +Fe or –Fe+$FePO_4$ conditions. E, *SlFRDL1* expression in AC and *SlSTOP1* KO lines under +Fe or –Fe+$FePO_4$ condition. Tomato seedlings were cultured hydroponically for 14 d, and the treatment solution was renewed every other day. All data are presented as means±SD (n=4 biological replicates) with different letters indicating significant differences among treatments at P≤0.05 level by ANOVA analysis.

and D), suggesting post-transcriptional regulation of SlSTOP1 protein accumulation.

This observation aligns with established mechanisms of STOP1 regulation under acidic pH conditions during aluminum stress (Huang and Ma 2024) and Fe-dependent low Pi responses mediated through the STOP1-ALMT1 pathway (Godon *et al.* 2019). Notably, our –Fe+$FePO_4$ treatment induced significant rhizosphere acidification (Fig. 2-A and B). To directly test pH dependency, we conducted a pH gradient experiment demonstrating that Fe deficiency failed to induce *SlFRDL1* expression at pH 7.5 (Fig. 7-E). In contrast, *SlFER* maintained Fe deficiency responsiveness at neutral pH despite reduced expression levels at higher pH (Fig. 7-F). Consistent with *SlFRDL1* expression patterns under varying pH conditions, citrate secretion decreased progressively as pH increased (Fig. 7-G). Additionally, *SlAHA2* expression was induced by elevated pH but no further induction under Fe deficiency at pH 7.5 (Fig. 7-H). These results indicate that Fe deficiency activates SlSTOP1–SlFRDL1 pathway to promote citrate secretion in a pH-dependent manner.

4. Discussion

4.1. Coordinated regulation of Fe solubilization through proton excretion and organic acid secretion

In Strategy I plants, Fe acquisition typically depends on three hallmark processes: H^+-ATPase-mediated rhizosphere acidification, ferric chelate reductase activity, and IRT1-mediated Fe^{2+} uptake (Riaz and Guerinot 2021). However, emerging evidence indicates these mechanisms become less effective under neutral or alkaline soil conditions (Susin *et al.* 1996; Lucena *et al.* 2007; Waters *et al.* 2018). While phenolic compound exudation has been implicated in Fe mobilization under alkaline pH in Strategy I species (Gautam *et al.* 2021), the relative contributions of root exudates to Fe acquisition in weakly acidic environments remain poorly characterized. Here, we revealed that root exudates contribute substantially to solubilize rhizosphere Fe, thereby alleviating Fe deficiency symptoms (Fig. 1).

Our findings reveal distinct mechanisms operating in weakly acidic conditions (pH 5.0–6.0). Chemical dissolution assays demonstrated that proton-mediated $FePO_4$ solubilization shows negligible effects above pH 5, with H^+ exhibiting consistently lower solubilization capacity compared to organic acids across all tested pH ranges (Fig. 2). Notably, we identified pH-dependent ligand specificity among organic acids, with citrate and oxalate displaying superior Fe-mobilizing capacity below pH 6 (Fig. 2-A and B). Citrate emerged as particularly effective in the pH 5.0–6.0 range, solubilizing remarkably more Fe from $FePO_4$ than equivalent proton concentrations (Fig. 2-C). This pH-dependent synergy between organic acid secretion and moderate proton extrusion enables efficient Fe acquisition

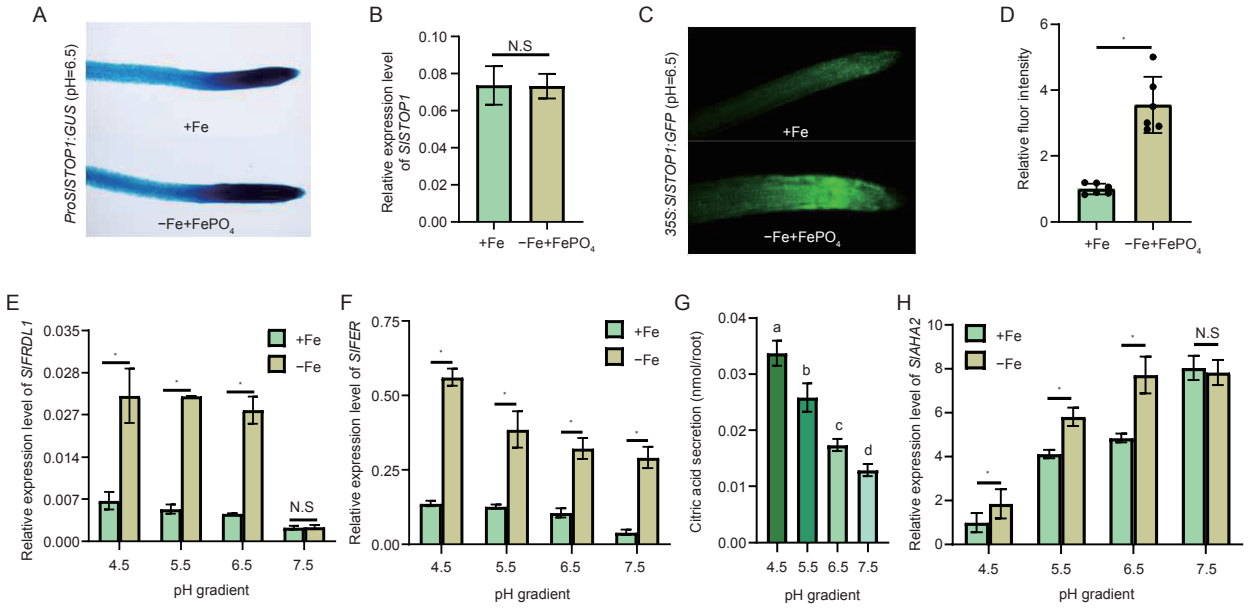

Fig. 7 Fe deficiency-activated SlSTOP1–SlFRDL1 module is dependent on acidic environment. A, *SlSTOP1* expression was not responsive to Fe deficiency. 14-d-old *ProSlSTOP1::GUS* reporter transgenic lines were subjected to Fe sufficiency (+Fe) or Fe deficiency with $FePO_4$ supplement (–Fe+ $FePO_4$) for 3 d. B, qRT-PCR analysis of *SlSTOP1* expression under Fe sufficiency (+Fe) or Fe deficiency with $FePO_4$ supplement (–Fe+ $FePO_4$) for 3 d. C, SlSTOP1 proteins were induced by –Fe+$FePO_4$ conditions. The 14-d-old *35S::SlSTOP1::GFP* transgenic reporter lines were subjected to Fe sufficiency (+Fe) or Fe deficiency with $FePO_4$ supplement (–Fe+ $FePO_4$) for 3 d. GFP fluorescence was observed by fluorescence microscope. D, quantification of GFP fluorescence from recombinant SlSTOP1-GFP protein in root tips. E and F, the *SlFRDL1* expression (E) and *SlFER* expression (F) with Fe sufficiency (+Fe) or deficiency (–Fe) at different pH conditions. G, citric acid secretion at different pH conditions. H, the relative expression levels of *SlAHA2* with or without Fe sufficiency at different pH conditions. Asterisks and different letter means significant difference. Asterisk indicated significant difference. Means±SD (*n*=6 biological replicates) with asterisks indicated significant differences among treatments at $P \leq 0.05$ level by Tukey's test.

from sparingly soluble Fe sources at circumneutral pH. These results establish a mechanistic framework where root exudates, particularly citrate in the critical pH 5–6 range, play a dominant role in Fe solubilization, compensating for the limited direct contribution of protons under weakly acidic conditions.

4.2. SlSTOP1–SlFRDL1 module controls Fe deficiency-induced root citrate secretion for Fe acquisition

We functionally characterized *SlFRDL1* with respect to Fe deficiency-induced citrate secretion. This is supported by the following pieces of evidence. First, the expression of *SlFRDL1* could be induced greatly by Fe deficiency (Fig. 3-A and B). Second, SlFRDL1 mediates citrate exudation when expressed in oocytes (Fig. 3-D and F). Third, *SlFRDL1* knockout mutants displayed exacerbated young leaf chlorosis and lower Fe content compared to WT plants, which is accompanied by reduced citrate secretion from roots (Fig. 4). Therefore, we concluded that SlFRDL1 is a Fe deficiency inducible citrate transporter that mediates citrate secretion.

We further demonstrated that SlSTOP1 is a major TF that regulates *SlFRDL1* expression in response to Fe deficiency. STOP1 and its homologs have been well characterized as the master regulators activating transcription of genes involved in proton tolerance (Iuchi *et al.* 2007; Fan *et al.* 2015), Al resistance (Sawaki *et al.* 2009; Zhu *et al.* 2024a), and responses to mineral nutrition deficiency (Balzergue *et al.* 2017; Tian *et al.* 2021; Ye *et al.* 2021; Liu *et al.* 2025). In this study, the findings that SlSTOP1 could directly bind to the promoter of *SlFRDL1* and activate its transcription indicate that SlSTOP1 regulates *SlFRDL1* expression (Fig. 5). Moreover, *Slstop1* mutants displayed leaf chlorosis symptom same as *Slfrdl1* mutants in –Fe+$FePO_4$, and the *SlFRDL1* expression induction by Fe deficiency was significantly repressed in *Slstop1* mutants compared to WT plants (Fig. 6). Notably, the expression induction of *SlFRDL1* was not completely repressed, suggesting that there are other regulators contribute to *SlFRDL1* expression under Fe deficiency. Notably, *Slfrdl1* and *Slstop1* mutants exhibited decreased shoot Fe levels under Fe-sufficient conditions, implying their involvement in Fe translocation process. Together, these results indicate that SlSTOP1–SlFRDL1 module controls Fe deficiency-induced root citrate secretion for Fe acquisition.

4.3. Possible regulatory mechanisms of SlSTOP1 activation under Fe deficiency

Studies on Arabidopsis STOP1 activation in response to Al stress have revealed posttranscriptional and posttranslational regulatory mechanisms of STOP1 (Huang and Ma 2024). Recently, an Al receptor has been characterized that binds intracellular Al to oxidatively modify RAE1, thereby degrading RAE1 (Ding *et al.* 2024; Ryan and Yang 2024). RAE1 is a F-box protein constituting SCF E3 ligase that ubiquitinates

STOP1 to facilitate STOP1 degradation (Zhang *et al.* 2019). However, it is unknown how STOP1 and its homologs in other plant species are activated in response to other stressors. Here, we demonstrated that SlSTOP1 could be activated by Fe deficiency as evidenced by the expression induction of *SlFRDL1* and citrate secretion. Interestingly, this activation appeared to be dependent on environmental pH condition, because at alkaline pH, the expression induction of *SlFRDL1* was abolished but *FER*, the core regulator of Fe deficiency response, remained induced (Fig. 7). Based on these pieces of information, we hypothesize that acidic environment is necessary for activating STOP1 proteins.

Multiple lines of experimental evidence converge to support the pivotal role of acidic environments in STOP1 activation. First, the initial identification of STOP1 through *Arabidopsis* proton-sensitivity mutant screening implicated its association with low pH signaling (Iuchi *et al.* 2007). Second, subsequent studies demonstrated pH-dependent regulation mechanisms: low pH independently induces *ALMT1* expression without aluminum involvement (Le Poder *et al.* 2022), while acidic conditions directly activate STOP1 to modulate *NRT1.1* expression (Ye *et al.* 2021). Third, phosphorus (Pi) deficiency-induced STOP1 activation observed in previous studies (Balzergue *et al.* 2017; Godon *et al.* 2019) inherently occurred under acidic conditions, with recent evidence highlighting the essentiality of NH_4^+, a proton-releasing nitrogen source for this process (Tian *et al.* 2021). These collective findings establish low pH as a prerequisite for STOP1 activation across diverse stress responses.

Paradoxically, our discovery of Fe deficiency-induced SlSTOP1 activation in tomato appears contradictory to established mechanisms. Earlier reports emphasized the indispensability of Fe for STOP1 accumulation and *ALMT1* induction under Pi deficiency (Godon *et al.* 2019), and revealed synergistic regulation of STOP1 by Fe and Al (Le Poder *et al.* 2022). This discrepancy suggests two non-mutually exclusive possibilities. One is that distinct stress signals may converge on common downstream effectors that interface with pH signaling to co-regulate STOP1. The other is that stress-specific metabolites (e.g., Fe-chelating compounds or Al^{3+} analogs) could mimic proton toxicity under particular conditions. Resolving this paradox warrants systematic investigation into stress-specific signaling crosstalk, particularly focusing on pH-sensing mechanisms, ion homeostasis networks, and post-translational modifications of STOP1 across plant species.

5. Conclusion

Under Fe-deficient conditions, the expression of *SlFRDL1*, encoding a citrate transporter protein, is significantly upregulated. This transporter facilitates citrate exudation from the root apex, which in concert with H^+-ATPase-mediated H^+ extrusion possibly *via* SlAHA2/4, contributing to solubilizing sparingly available Fe in the rhizosphere. Molecular characterization revealed that this transcriptional activation occurs through direct binding of the transcription factor SlSTOP1 to the *SlFRDL1* promoter region. Notably, the SlSTOP1–SlFRDL1 regulatory pathway demonstrates proton-sensitivity during Fe deficiency. Our study elucidates the crucial role of the SlSTOP1–SlFRDL1 module in governing Fe solubilization in response to environmental pH variations (Fig. 8), offering novel mechanistic insights into pH-dependent Fe mobilization processes in plants.

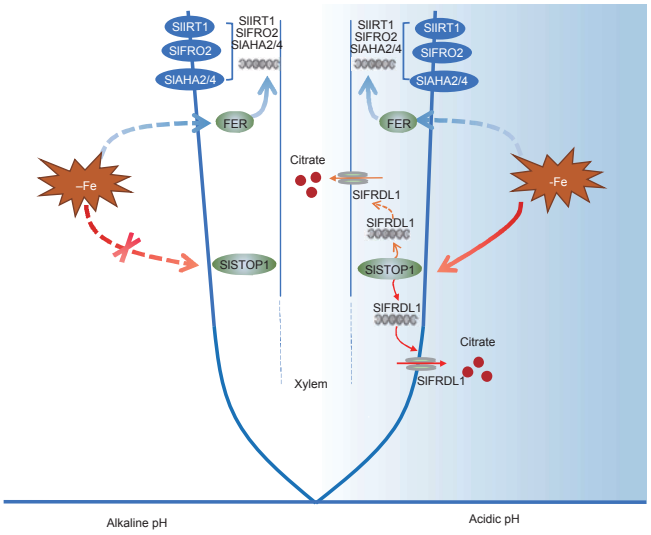

Fig. 8 A working model of the SlSTOP1–SlFRDL1 regulatory pathway mediating proton-responsive citrate exudation under Fe deficiency. Under both alkaline and acidic pH conditions, Fe deficiency activates the canonical FER-mediated iron acquisition mechanism, which includes three key components: (1) H^+-ATPase-mediated rhizosphere acidification, (2) ferric chelate reductase (FCR)-catalyzed Fe^{3+} reduction, and (3) IRT1-mediated Fe^{2+} uptake. Notably, under acidic pH conditions specifically, Fe deficiency additionally promotes SlSTOP1 protein accumulation, which in turn transcriptionally activates SlFRDL1. The SlFRDL1 protein, expressed predominantly at the root apex, facilitates citrate exudation into the rhizosphere. The released citrate chelates iron from sparingly soluble $FePO_4$, enhancing iron bioavailability. Importantly, this SlSTOP1–SlFRDL1 regulatory pathway remains inactive under alkaline pH conditions. SlFRDL1 may also expressed at vasculature where it facilitates Fe translocation in xylem.

Acknowledgements

This work was financially supported by the Joint Agricultural Project of Department of Science and Technology of Yunnan Province, China (202401BD070001-010), the National Natural Science Foundation of China (32372803) and the Science and Technology Major Project of Yunnan Province Science and Technology Department, China (202502AE090025 to J. Y.).

Declaration of competing interest

The authors declare that they have no conflict of interest.

Declaration of generative AI and AI-assisted technologies in the writing process

The authors declare that they did not use AI in the preparation and writing of this manuscript.

Appendices associated with this paper are available at https://doi.org/10.1016/j.jia.2025.12.072

References

Awad F, Romheld V, Marschner H. 1994. Effect of root exudates on mobilization in the rhizosphere and uptake from by wheat plants. *Plant and Soil*, **165**, 213–218.

Balzergue C, Dartevelle T, Godon C, Laugier E, Meisrimler C, Teulon J M, Creff A, Bissler M, Brouchoud C, Hagege A, Muller J, Chiarenza S, Javot H, Becuwe-Linka N, David P, Peret B, Delannoy E, Thibaud M C, Armengaud J, Abel S, *et al.* 2017. Low phosphate activates STOP1-ALMT1 to rapidly inhibit root cell elongation. *Nature Communications*, **8**, 15300.

Briat J F, Dubos C, Gaymard F. 2015. Iron nutrition, biomass production, and plant product quality. *Trends in Plant Science*, **20**, 33–40.

Chen W W, Zhu H H, Wang J Y, Han G H, Huang R N, Hong Y G, Yang J L. 2022. Comparative physiological and transcriptomic analyses reveal altered Fe-deficiency responses in tomato epimutant *Colorless non-ripening*. *Frontiers in Plant Science*, **12**, 796893.

Chen Y T, Wang Y, Yeh K C. 2017. Role of root exudates in metal acquisition and tolerance. *Current Opinion in Plant Biology*, **39**, 66–72.

Ding Z J, Xu C, Yan J Y, Wang Y X, Cui M Q, Yuan J J, Wang Y N, Li G X, Wu J X, Wu Y R, Xu J M, Li C X, Shi Y Z, Mao C Z, Guo J T, Zhou J M, Benhamed M, Harberd N P, Zheng S J. 2024. The LRR receptor-like kinase ALR1 is a plant aluminum ion sensor. *Cell Research*, **34**, 281–294.

Durrett T P, Gassmann W, Rogers E E. 2007. The FRD3-mediated efflux of citrate into the root vasculature is necessary for efficient iron translocation. *Plant Physiology*, **144**, 197–205.

Fan W, Lou H Q, Gong Y L, Liu M Y, Cao M J, Liu Y, Yang J L, Zheng S J. 2015. Characterization of an inducible C_2H_2-type zinc finger transcription factor VuSTOP1 in rice bean (*Vigna umbellata*) reveals differential regulation between low pH and aluminum tolerance mechanisms. *New Phytologist*, **208**, 456–468.

Fujii M, Yokosho K, Yamaji N, Saisho D, Yamane M, Takahashi H, Sato K, Nakazono M, Ma J F. 2012. Acquisition of aluminium tolerance by modification of a single gene in barley. *Nature Communications*, **3**, 713.

Gautam C K, Tsai H H, Schmidt W. 2021. IRONMAN tunes responses to iron deficiency in concert with environmental pH. *Plant Physiology*, **187**, 1728–1745.

Godon C, Mercier C, Wang X, David P, Richaud P, Nussaume L, Liu D, Desnos T. 2019. Under phosphate starvation conditions, Fe and Al trigger accumulation of the transcription factor STOP1 in the nucleus of Arabidopsis root cells. *The Plant Journal*, **99**, 937–949.

Green L S, Rogers E E. 2004. FRD3 controls iron localization in Arabidopsis. *Plant Physiology*, **136**, 2523–2531.

Huang C F, Ma Y. 2024. Aluminum resistance in plants: A critical review focusing on STOP1. *Plant Communications*, **6**, 101200.

Iuchi S, Koyama H, Iuchi A, Kobayashi Y, Kitabayashi S, Kobayashi Y, Ikka T, Hirayama T, Shinozaki K, Kobayashi M. 2007. Zinc finger protein STOP1 is critical for proton tolerance in Arabidopsis and coregulates a key gene in aluminum tolerance. *Proceedings of the National Academy of Sciences of the United States of America*, **104**, 9900–9905.

Jin C W, Du S T, Shamsi I H, Luo B F, Lin X Y. 2011. NO synthase-generated NO acts downstream of auxin in regulating Fe-deficiency-induced root branching that enhances Fe-deficiency tolerance in tomato plants. *Journal of Experimental Botany*, **62**, 3875–3884.

Jin C W, You G Y, He Y F, Tang C, Wu P, Zheng S J. 2007. Iron deficiency-induced secretion of phenolics facilitates the reutilization of root apoplastic iron in red clover. *Plant Physiology*, **144**, 278–285.

Jin J F, Zhu H H, He Q Y, Li P F, Fan W, Xu J M, Yang J L, Chen W W. 2022. The tomato transcription factor SlNAC063 is required for aluminum tolerance by regulating SlAAE3-1 expression. *Frontiers in Plant Science*, **13**, 826954.

JonesD L, Darrah P R, Kochian L V. 1996. Critical evaluation of organic acid mediated iron dissolution in the rhizosphere and its potential role in root iron uptake. *Plant and Soil*, **180**, 57–66.

Kobayashi T, Nishizawa N K. 2012. Iron uptake, translocation, and regulation in higher plants. *Annuanl Review of Plant Biology*, **63**, 131–152.

Liang G. 2022. Iron uptake, signaling, and sensing in plants. *Plant Communications*, **3**, 100349.

Liu G, Chen Q, Li D, Mai H, Zhou Y, Lin M, Feng X, Lin X, Lu X, Chen K, Tian J, Liang C. 2025. GmSTOP1-3 increases soybean manganese accumulation under phosphorus deficiency by regulating *GmMATE2/13* and *GmZIP6/GmIREG3*. *Plant Cell and Environment*, **48**, 1812–1828.

Liu J P, Magalhaes J V, Shaff J, Kochian L V. 2009. Aluminum-activated citrate and malate transporters from the MATE and ALMT families function independently to confer Arabidopsis aluminum tolerance. *The Plant Journal*, **57**, 389–399.

Liu M Y, Lou H Q, Chen W W, Pineros M A, Xu J M, Fan W, Kochian L V, Zheng S J, Yang J L. 2018. Two citrate transporters coordinately regulate citrate secretion from rice bean root tip under aluminum stress. *Plant Cell and Environment*, **41**, 809–822.

Lucena C, Romera F J, Rojas C L, Garcia M, Alcantara E, Perez-Vicente R. 2007. Bicarbonate blocks the expression of several genes involved in the physiological responses to Fe deficiency of Strategy I plants. *Functional Plant Biology*, **34**, 1002–1009.

Mori S. 1999. Iron acquisition by plants. *Current Opinion in Plant Biology*, **2**, 250–253.

Nozoye T, Nagasaka S, Kobayashi T, Takahashi M, Sato Y, Sato Y, Uozumi N, Nakanishi H, Nishizawa N K. 2011. Phytosiderophore efflux transporters are crucial for iron acquisition in graminaceous plants. *Journal of Biological Chemistry*, **286**, 5446–5454.

Oburger E, Gruber B, Schindlegger Y, Schenkeveld W D C, Hann S, Kraemer S M, Wenzel W W, Puschenreiter M. 2014. Root exudation of phytosiderophores from soil-grown wheat. *New Phytologist*, **203**, 1161–1174.

Piñeros M A, Cancado G M, Kochian L V. 2008. Novel properties of the wheat aluminum tolerance organic acid transporter (TaALMT1) revealed by electrophysiological characterization in *Xenopus* oocytes: Functional and structural implications. *Plant Physiology*, **147**, 2131–2146.

Le Poder L, Mercier C, Fevrier L, Duong N, David P, Pluchon S, Nussaume L, Desnos T. 2022. Uncoupling aluminum toxicity from aluminum signals in the STOP1 pathway. *Fronties in Plant Science*, **13**, 785791.

Rajniak J, Giehl R F H, Chang E, Murgia I, von Wiren N, Sattely E S. 2018. Biosynthesis of redox-active metabolites in response to iron deficiency in plants. *Nature Chemical Biology*, **14**, 442–450.

Riaz N, Guerinot M L. 2021. All together now: regulation of the iron deficiency response. *Journal of Experimental Botany*, **72**, 2045–2055.

Rogers E E, Wu X, Stacey G, Nguyen H T. 2009. Two MATE proteins play a role in iron efficiency in soybean. *Journal of Plant Physiology*, **166**, 1453–1459.

Römheld V, Marschner H. 1986. Evidence for a specific uptake system for iron phytosiderophores in roots of grasses. *Plant Physiology*, **80**, 175–180.

Rosenkranz T, Oburger E, Baune M, Weber G, Puschenreiter M. 2021. Root exudation of coumarins from soil-grown *Arabidopsis thaliana* in response to iron deficiency. *Rhizosphere*, **17**, 100296.

Ryan P R, Yang J. 2024. Sensing the toxic aluminum cations in acidic soils, *Cell Research*, **34**, 269–270.

Santi S, Schmidt W. 2009. Dissecting iron deficiency-induced proton extrusion in Arabidopsis roots. *New Phytologist*, **183**, 1072–1084.

Sawaki Y, Iuchi S, Kobayashi Y, Kobayashi Y, Ikka T, Sakurai N, Fujita M, Shinozaki K, Shibata D, Kobayashi M, Koyama H. 2009. STOP1 regulates multiple genes that protect Arabidopsis from proton and aluminum toxicities. *Plant Physiology*, **150**, 281–294.

Schmid N B, Giehl R F H, Doell S, Mock H P, Strehmel N, Scheel D, Kong X, Hider R C, von Wiren N. 2014. Feruloyl-coA 6′-hydroxylase1-dependent coumarins mediate iron acquisition from alkaline substrates in Arabidopsis. *Plant Physiology*, **164**, 160–172.

Susin S, Abadia A, Gonzalez-Reyes J A, Lucena J J, Abadia J.1996. The pH requirement for in vivo activity of the iron deficiency-induced ''Turbo'' ferric chelate reductase — A comparison of the iron-deficiency-induced iron reductase activities of intact plants and isolated plasma membrane fractions in sugar beet. *Plant Physiology*, **110**, 111–123.

Tian W H, Ye J Y, Cui M Q, Chang J B, Liu Y, Li G X, Wu Y R, Xu J M, Harberd N P, Mao C Z, Jin C W, Ding Z J, Zheng S J. 2021. A transcription factor STOP1-centered pathway coordinates ammonium and phosphate acquisition in Arabidopsis. *Molecular Plant*, **14**, 1554–1568.

Tsai H H, Rodriguez-Celma J, Lan P, Wu Y C, Velez-Bermudez I C,

Schmidt W. 2018. Scopoletin 8-hydroxylase-mediated fraxetin production is crucial for iron mobilization. *Plant Physiology*, **177**, 194–207.

Tsutsui T, Yamaji N, Ma J F. 2011. Identification of a cis-acting element of ART1, a C2H2-type zinc-finger transcription factor for aluminum tolerance in rice. *Plant Physiology*, **156**, 925–931.

Waters B M, Amundsen K, Graef G. 2018. Gene expression profiling of iron deficiency chlorosis sensitive and tolerant soybean indicates key roles for phenylpropanoids under alkalinity stress. *Frontiers in Plant Science*, **9**, 10.

Yang J L, Fan W, Zheng S J. 2019. Mechanisms and regulation of aluminum-induced secretion of organic acid anions from plant roots. *Journal of Zhejiang University SCIENCE B*, **20**, 513–527.

Yang X Y, Yang J L, Zhou Y, Piñeros M A, Kochian L V, Li G X, Zheng S J. 2011. A *de novo* synthesis citrate transporter, *Vigna umbellata* multidrug and toxic compound extrusion, implicates in Al-activated citrate efflux in rice bean (*Vigna umbellata*) root apex. *Plant Cell and Environment*, **34**, 2138–2148.

Ye J Y, Tian W H, Zhou M, Zhu Q Y, Du W X, Zhu Y X, Liu X X, Lin X Y, Zheng S J, Jin C W. 2021. STOP1 activates NRT1.1-mediated nitrate uptake to create a favorable rhizospheric pH for plant adaptation to acidity. *The Plant Cell*, **33**, 3658–3674.

Yokosho K, Yamaji N, Fujii-Kashino M, Ma J F. 2016. Retrotransposon-mediated aluminum tolerance through enhanced expression of the citrate transporter *OsFRDL4*. *Plant Physiology*, **172**, 2327–2336.

Zhang Y, Zhang J, Guo J L, Zhou F L, Singh S, Xu X, Xie Q, Yang Z B, Huang C F. 2019. F-box protein RAE1 regulates the stability of the aluminum-resistance transcription factor STOP1 in Arabidopsis. *Proceedings of the National Academy of Sciences of the United States of America*, **116**, 319–327.

Zhu H H, Chen W W, Yang Z A, Zeng C, Fan W, Yang J. 2024a. SlSTOP1-regulated *SlHAK5* expression confers Al tolerance in tomato by facilitating citrate secretion from roots. *Horticulture Research*, **11**, uhae282.

Zhu H H, Han G H, Wang J Y, Xu J M, Hong Y G, Huang L, Zheng S J, Yang J L, Chen W W. 2023. CG hypermethylation of the bHLH39 promoter regulates its expression and Fe deficiency responses in tomato roots. *Horticulture Research*, **10**, uhad104.

Zhu H H, Wang J Y, Huang R N, Yang Z, Fan W, Huang L, Yang J, Chen W. 2024b. Epigenetic modification of a pectin methylesterase gene activates apoplastic iron reutilization in tomato roots. *Plant Physiology*, **195**, 2339–2353.

Zhu H H, Wang J Y, Jiang D, Hong Y G, Xu J M, Zheng S J, Yang J L, Chen W W. 2022. The miR157-SPL-CNR module acts upstream of bHLH101 to negatively regulate iron deficiency responses in tomato. *Journal of Integrative Plant Biology*, **64**, 1059–1075.